



Humic Acid-Modified Magnetite Nanoparticles for Removing $[\text{AuCl}_4]^-$ in Aqueous Solutions

Soerja Koesnarpadi^{a,*}, Nanang Tri Widodo^a, Achmad Maulana^a

^a Department of Chemistry, Mathematics and Natural Sciences, Universitas Mulawarman, Samarinda, Indonesia

*Corresponding author: soerja.koes@gmail.com

<https://doi.org/10.14710/jksa.25.1.27-33>

Article Info

Article history:

Received: 26th July 2021
 Revised: 22nd January 2022
 Accepted: 24th January 2022
 Online: 31st January 2022

Keywords:

Humic acid; modified; magnetite nanoparticle; removal; $[\text{AuCl}_4]^-$

Abstract

Humic acid-modified magnetite nanoparticle (MnP-HA) has been synthesized using the co-precipitation method and applied for removal of $[\text{AuCl}_4]^-$. Modifying of MnP-HA was prepared with the mass ratio of MnP-HA=10:1 and 10:3. The HA was extracted from peat soil of Sambutan Village, East Kalimantan, Indonesia, by the recommended procedure of the International Humic Substances Society (IHSS). The saturation magnetization of MnP-HA was decreased compared to unmodified MnP. The interaction between MnP and HA was occurred due to the chemical bond between Fe from MnP with the carboxylic group from HA. The coating HA on the surface of MnP unchanged the formation of the crystal structure of MnP and increased the particle size. The optimum removal of $[\text{AuCl}_4]^-$ on MnP and MnP-HA materials was optimum at pH 3.0. The Langmuir isotherm model with sorption capacity was 0.23, 4.85, and 4.65 mol g^{-1} for MnP, MnP-HA=10:1, and 10:3, respectively. Using a pseudo-second-order equation, the degradation of the kinetics model of $[\text{AuCl}_4]^-$ on MnP, MnP-HA=10:1 and 10:3 with adsorption rate constant (*k*) were 0.02, 0.07, and 0.06 $\text{g}\cdot\text{mol}^{-1}\cdot\text{min}^{-1}$.

1. Introduction

Gold is a metal that has high value because of its many utilizations. The deposition of gold (Au) metal is naturally in areas rich in peat soil, such as tropical peat soil in Kalimantan, Indonesia [1]. Due to the low concentration in nature, the extraction of Au is not an easy and cheap effort [2]. In some cases, the contents of Au in electronic Printed Circuit Board (PCB) wastes are higher than that in the ore itself [3]. Economically, recovery of Au from secondary sources such as electronic waste is more desirable than natural ore. Various methods that have been employed for the recovery of Au are co-precipitation [4], ion exchange [5], solvent extraction [6], and adsorption [7]. Among these methods, adsorption is one method of efficient, easily separated, and can be regenerated and reused [8].

Magnetite nanoparticle (MnP) is ferrite with the inverse spinel structure, nanosize, non-toxic, and therefore has many applications [9, 10]. They are widely used as nano sorbents not only in water-treatment

technologies [11] but also in biomedical applications [12] or analytical chemistry [13] due to their excellent sorption ability, good mechanical properties, and facile separability with a simple magnetic process [9]. Unfortunately, magnetite nanoparticles are susceptible to air oxidation and easily aggregated in an aqueous solution. Thus, the stabilization of magnetite is desirable [14, 15]. Hence, surface modification is essential to enhance the stability of magnetite nanoparticles [16].

Humic acid (HA) is an essential fraction of natural macromolecular organics and contains a multi-functional group, with the predominant functional groups being carboxyl and hydroxyl groups. The functional groups on HA possess different abilities in binding metal ions through complex formation [10, 14]. Humic acids can form stabilizing surfaces on MnP can effectively prevent the adhesion of colliding particles during thermal motion [17]. The coating HA and MnP have influenced the sorption properties of MnP because the bonding of HA gives a functional group on MnP, thus essentially altering the surface properties. Interaction

between HA and MnP has enhanced the stability of nanodispersion by preventing their aggregation [18, 19].

Recently, several studies have been conducted on the sorption of $[\text{AuCl}_4]^-$ effectively on humate substances, e.g., humin [20], humic acids [21], and fulvic acid-magnetite [22]. In this study, Further detail MnP-HA has been prepared with the mass ratio of MnP:HA =10:1 and 10:3, then applied to removal of $[\text{AuCl}_4]^-$. The functional groups, crystal structure, magnetic properties, and size distribution on MnP, MnP-HA=10:1, and 10:3 were characterized. The effect of pH, contact time, and initial concentration of removal AuCl_4^- were also investigated.

2. Methodology

2.1. Materials and Instrumentations

Peat soil from Sambutan village, Samarinda, East Kalimantan. The reagents of analytical grade, i.e., $\text{FeCl}_3 \cdot 6\text{H}_2\text{O}$, $\text{FeSO}_4 \cdot 7\text{H}_2\text{O}$, NH_4OH 25%, HCl , HNO_3 , HF , NaOH , $[\text{AuCl}_4]^-$ were obtained from Merck and N_2 . VSM type Oxford VSM 1.2 H, FT-IR spectrometer 8201 PC Shimadzu, X-ray diffractometer Shimadzu using $\text{CuK}\alpha$ radiation ($\lambda=1.5406 \text{ \AA}$) operated at 40kV and 30 mA. Scanning electron microscopy JEOL SSM-6510 LA, Atomic Absorption Spectrometer Perkin Elmer 3110.

2.2. Extraction of Humic Acid (HA)

Dry peat soil was added into NaOH solution 1.0 M with a weight (g) and NaOH volume (mL) ratio of 1:10 and then shaken for 24 h under a nitrogen atmosphere. The mixture was centrifuged at the rate of 2500 rpm for 30 min. After filtration, the supernatant was added 6 M HCl dropwise until pH 1 and followed by centrifugation at 2500 rpm for 30 min to precipitate crude HA. This crude HA was purified by a mixed solution consisting of 0.1 M HCl and 0.3 M HF with shaking at room temperature for 24 h. The resulting mixture was centrifuged at 2500 rpm for 30 min and the separated suspended material from the supernatant. This purification procedure was repeated to obtain a clear transparent supernatant.

2.3. Synthesis HA Modified MnP

MnP-HA was synthesized by the co-precipitation method by dissolving 1.525 g $\text{FeCl}_3 \cdot 6\text{H}_2\text{O}$ and 1.05 g $\text{FeSO}_4 \cdot 7\text{H}_2\text{O}$, respectively, into 25 mL of distilled water. The two solutions were heated at 90°C , and into this mixed solution, NH_4OH 25% was added until pH 11, and then 0.5 g of HA sodium salt, which was dissolved in 12.5 mL of distilled water, was added rapidly. The mixture was stirred at 90°C for 30 min and then cooled to room temperature. The black precipitate was separated from the solution and washed with distilled water until neutral pH was reached. The bare MnP was prepared with the same method as MnP-HA, except there was no HA addition.

2.4. Characterization of HA, MnP, and MnP-HA

The determination of total acidity and carboxyl content of HA and MnP-HA were carried out using $\text{Ba}(\text{OH})_2$ and $\text{Ca}(\text{CH}_3\text{COO})_2$ method [23]. The functional

groups of HA, MnP, and MnP-HA were characterized by Fourier transform spectrometer (FT-IR) 8201 PC Shimadzu. The crystal structure and size were analyzed by X-ray diffraction (XRD) Shimadzu using $\text{CuK}\alpha$ radiation ($\lambda=1.5406 \text{ \AA}$) operated at 40kV and 30 mA. Scanning electron microscopy (SEM) JEOL SSM-6510 LA is used to determine the surface morphology. The magnetic properties were analyzed by VSM type OXFORD VSM 1.2 H.

2.5. Removal of $[\text{AuCl}_4]^-$ on MnP-HA and MnP

2.5.1. The Effect of pH

Five mg of MnP was added into a series of 10 mL of $[\text{AuCl}_4]^-$ solution 25 mg L^{-1} varies from 2 to 7. The mixture was shaken for 60 min, and then the filtrate was separated and followed by an analysis of $[\text{AuCl}_4]^-$ content with Atomic Absorption Spectroscopy (Analytik Jena).

2.5.2. Sorption Kinetics

Five mg of MnP was added into a series of 10 mL of $[\text{AuCl}_4]^-$ at 25 mg L^{-1} and optimum pH, and each mixture was shaken at different contact times, ranging from 0 to 240 min. After filtration, the filtrate was analyzed of $[\text{AuCl}_4]^-$ content using Atomic Absorption Spectroscopy (Analytik Jena).

2.5.3. Sorption Isotherm

Five mg of MnP was added into a series of 10 mL of $[\text{AuCl}_4]^-$ solution at various concentrations ranging from 5 to 150 mg L^{-1} at optimum pH and contact time. The mixture was filtered, and the filtrate was analyzed its $[\text{AuCl}_4]^-$ content using AAS.

3. Results and Discussion

Humic acid-modified MnP were successfully coated using the co-precipitation method in alkaline conditions at pH 11 and heated at 90°C . The interaction between MnP and HA can be done under acidic or alkaline conditions. MnP is amphoteric, which can develop charge in the protonation and deprotonation reaction on the surface site of Fe-OH .

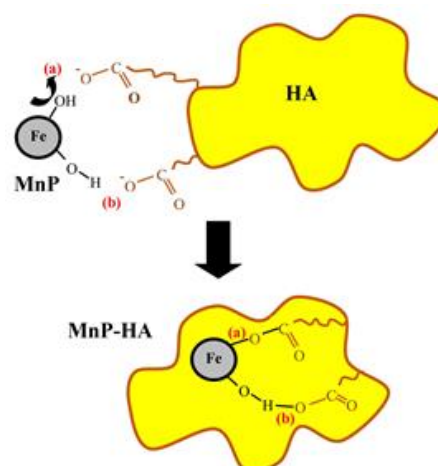


Figure 1. Illustration of interaction between MnP and HA under alkaline conditions, ligand-exchange (a) and hydrogen bond (b)

The illustration of the interaction between MnP and HA under alkaline conditions ($pH > pH_{pzc}$) is shown in Figure 1. The surface charge MnP is negative, the binding between MnP and HA is occurring due to ligand-exchange with the surface of hydroxyl and can form Fe-carboxylic bonds (a). The interaction of MnP between HA can occur through the hydrogen bond between the hydroxyl group of MnP and the oxygen atom on the carboxyl group of HA (b) [24, 25].

Table 1. Total acidity, carboxyl, and hydroxyl content HA and MnP-HA

Content (cmol kg ⁻¹)	Stevenson (1994)	HA	MnP-HA=10:1	MnP-HA=10:3
Total acidity	570-890	685	310	365
Carboxyl	150-570	334	62	98
Hydroxyphenolic	150-400	351	248	267

Based on the determination of total acidity and carboxyl content of HA and MnP-HA, this shows that carboxyl and hydroxyl content in HA would decrease after modified MnP, as shown in Table.1. This indicates that some HA carboxyl and hydroxyl groups were used to bond MnP.

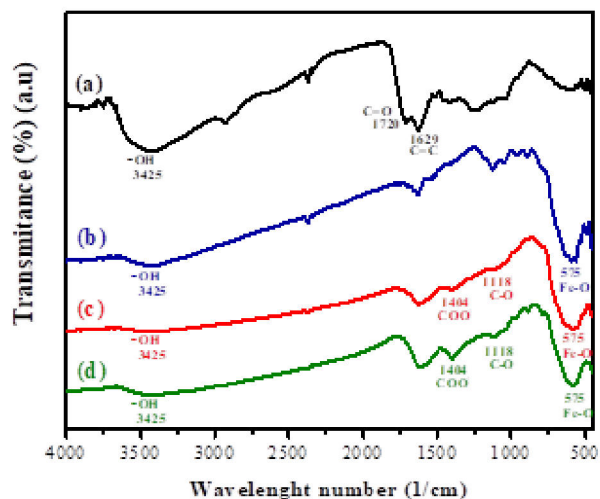


Figure 2. FTIR spectra of HA (a) MnP (b), MnP-HA=10:1(c) and MnP-HA=10:3 (d)

The FTIR spectra of HA from Sambutan Village, East Kalimantan, was the appearance of O-H stretching vibration at 3425 cm⁻¹, the functional group of C=O stretching vibration at 1720 cm⁻¹ and aromatic C=C stretching vibration and 1629 cm⁻¹ [26, 27]. The absorption bands for MnP at 3425 cm⁻¹ and 575 cm⁻¹ were O-H stretching of hydroxyl group and specific Fe-O stretching groups, respectively [19]. After HA modified MnP, new absorption C=O stretching vibration was shown at 1404 cm⁻¹ and C-O free carboxyl groups at 1118 cm⁻¹. This indicates that the stretching vibration of C=O and C-O of free carboxyl groups of HA interacted with

FeO of MnP. The FTIR spectra HA, MnP, and MnP-HA as shown in Figure 2.

The XRD pattern of MnP and MnP-HA were similar diffraction peaks at $2\theta = 30.1^\circ, 35.4^\circ, 43.1^\circ, 57.0^\circ, 62.68^\circ,$ and 74.5° which corresponded to peaks characteristic of inverse cubic spinel structure (JCPDS 65-3107) [14, 25]. The HA-modified MnP did not change the crystal structure of bare MnP but decreased XRD peak intensity. XRD diffractogram of MnP, MnP-HA=10:1, and MnP-HA=10:3 is shown in Figure 3.

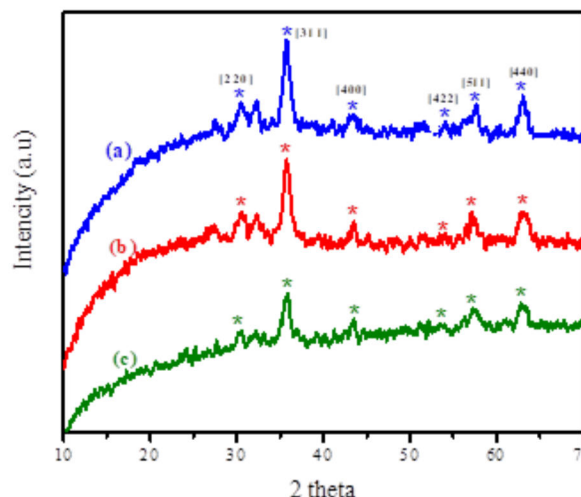


Figure 3. XRD diffractogram of MnP (a), MnP-HA=10:1 (b), and MnP-HA=10:3 (c)

The crystallite size was calculated using Debye-Scherrer equations. This result shows crystallite size decreased with the increased content of HA, indicating that the coating HA on MnP was successfully dispersed in a smaller size. The MnP-HA has a smaller crystallite size than MnP. Crystallite size was obtained using Debye-Scherrer equations of MnP, MnP-HA=10:1, and MnP-HA=10:3, as shown in Table.2.

Table 2. Crystallite size using Debye-Scherrer equations of MnP and MnP-HA

Materials	2 θ	FWHM (β)	Average crystalline size(d=nm)
MnP	35,69	0,587	13,455
MnP-HA=10:1	35,56	0,769	10,274
MnP-HA=10:3	35,71	0,844	9,357

Figure 4 shows the SEM image of HA, MnP, MnP-HA=10:1, and MnP-HA=10:3. The HA had an irregular shape structure with a smooth surface (Figure 5a), while MnP shows spherical homogenous-shaped with nanosize (Figure 5b). Morphology surface of MnP-HA=10:1 and MnP-HA=10:3 shows the surface of HA appeared to be modified by rough-bright spherical of MnP (Figure 3c and 3d) [27].

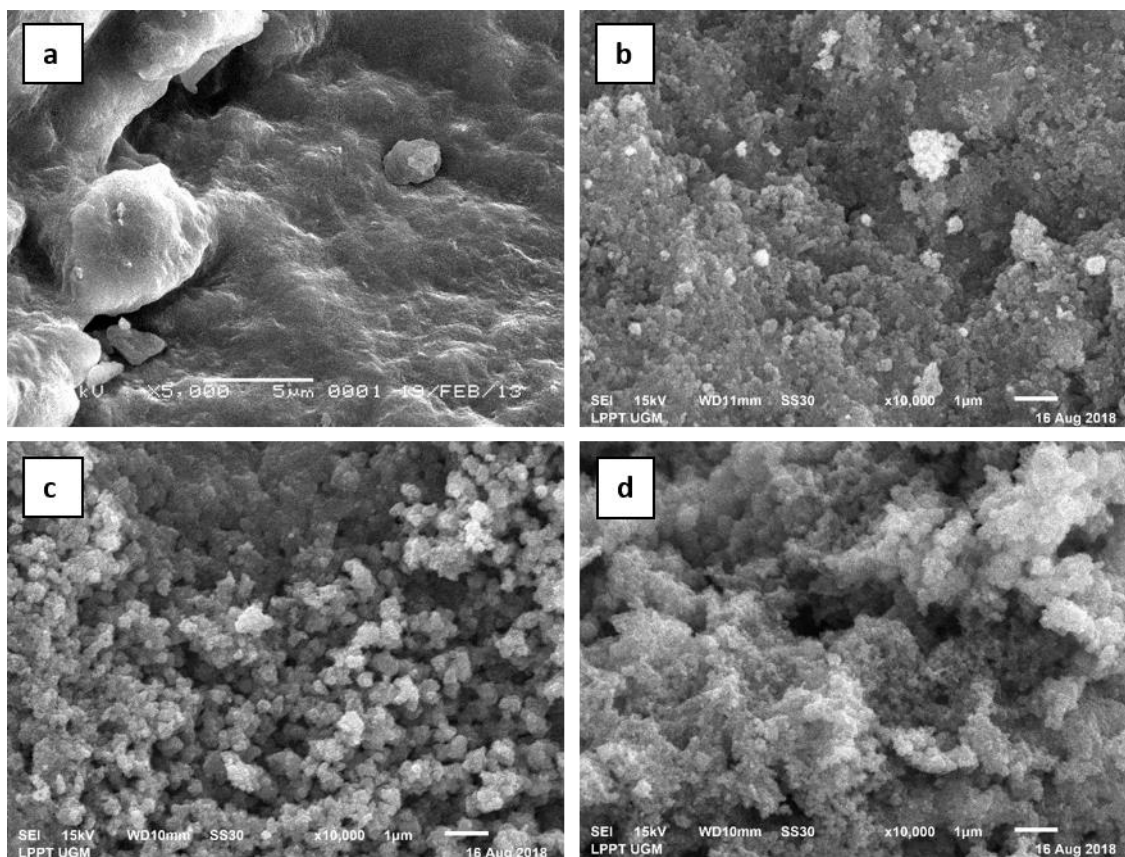


Figure 4. SEM image of HA 5000× magnification (a), MnP 10000× magnification (b), MnP-HA=10:1 10000× magnification (c), MnP-HA=10:3 10000× magnification (d)

The saturation magnetization value of MnP was 71.25 emu.g^{-1} , while MnP-HA=1:10 and MnP-HA=10:3 were 57.80 and 38.39 emu.g^{-1} , respectively. (Figure 5). The saturation magnetization of MnP decreased with the increased content of HA, but such a decrease was still adequate for the separation using magnetic field [17, 28].

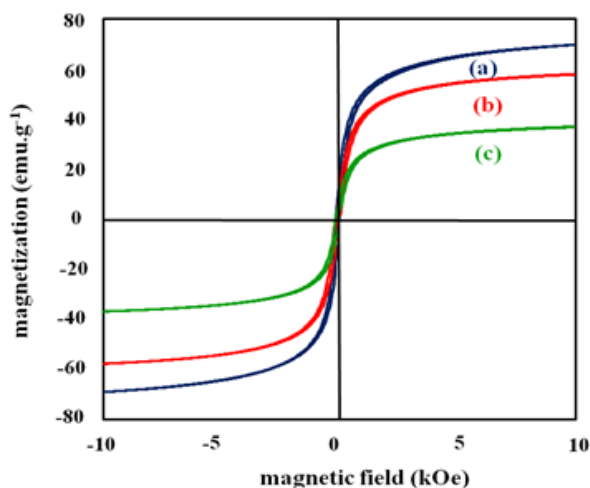


Figure 5. Magnetization curve of MnP (a), MnP-HA=10:1 (b) and MnP-HA=10:3 (c)

The $[\text{AuCl}_4]^-$ removal from MnP, MnP-HA=10:1 and 10:3, were influenced by pH, and optimum removal of $[\text{AuCl}_4]^-$ occurred at pH 3 as shown in Figure 6.

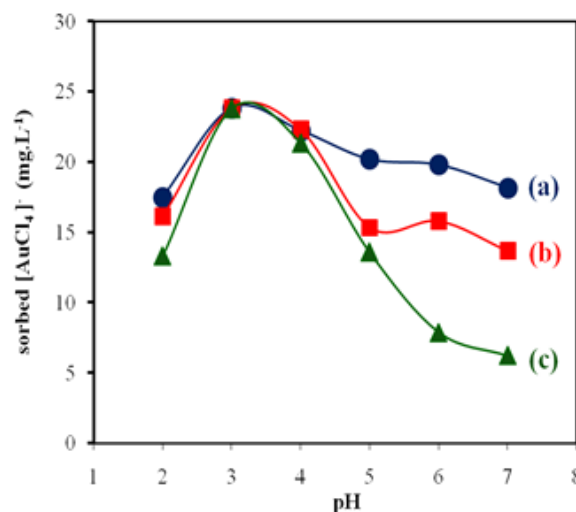


Figure 6. Effect of initial pH on removal of $[\text{AuCl}_4]^-$ using MnP (a), MnP-HA=10:1(b), and MnP-HA=10:3 (c)

At very acidic conditions (low pH < 3.0), adsorbent has less stability. This means, with the decreasing pH led to less percentage of sorbed $[\text{AuCl}_4]^-$. At pH 3.0, the carboxyl group in MnP-HA was protonated and led to the complete sorption with the negative species of $[\text{AuCl}_4]^-$ with hydrogen bonding. Above pH 3.0, more functional groups of MnP-HA were deprotonated to negatively charged. The repulsion between negatively charged MnP-HA and $[\text{AuCl}_4]^-$ causing the sorbed of $[\text{AuCl}_4]^-$ on MnP-HA was decreased with the increasing pH [17, 22].

The effect of contact time removal of $[\text{AuCl}_4]^-$ on MnP, MnP-HA=10:1 and 10:3 as shown in Figure 7. The removal was initially rapid at first 60 min and then slowed down with increasing contact time. In the early minutes, the carboxyl group of MnP-HA is the responsible functional group for the binding with $[\text{AuCl}_4]^-$. After equilibrium was reached, a decrease in the sorbed amount of $[\text{AuCl}_4]^-$ was observed.

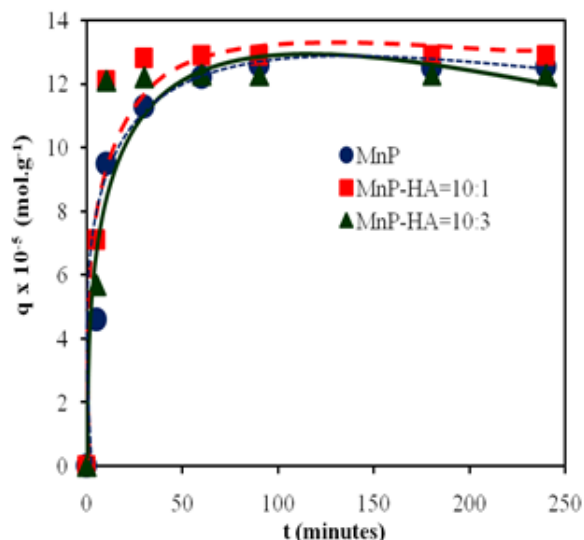


Figure 7. Effect of contact time on the removal of $[\text{AuCl}_4]^-$ using MnP, MnP-HA=10:1 and MnP-HA=10:3

The removal kinetics of $[\text{AuCl}_4]^-$ on MnP, MnP-HA=10 and 10:3 can be described by a pseudo-second-order equation as Eq (1), where q_t (mol g^{-1}) is the amount of $[\text{AuCl}_4]^-$ sorbed at a certain time t (minute), k (g/mol.min) is pseudo-second-order rate constant. If conditions $t=0$ ($q_t=0$) to t_e ($q_t=q_e$) [29].

$$\frac{t}{q_t} = \frac{1}{q_e} t + \frac{1}{k \cdot q_e^2} \quad (1)$$

A linear relationship with high correlation coefficients was observed, indicating the applicability of Ho's pseudo-second-order model, as shown in Table 3. The obtained k for removing $[\text{AuCl}_4]^-$ on MnP, MnP-HA=10:1 and 10:3 were 0.022, 0.077, and 0.057 $\text{g.mol}^{-1} \text{min}^{-1}$, respectively. The removal rate of $[\text{AuCl}_4]^-$ on MnP-HA was higher than on MnP.

Table 3. Kinetic parameters of the pseudo-first-order and pseudo-second-order for removal of $[\text{AuCl}_4]^-$ on MnP, MnP-HA=10:1 and 10:3

Models	Parameters	MnP	MnP-HA=10:1	MnP-HA=10:3
Lagergren's pseudo-first-order	R^2	0.853	0.738	0.645
	q_e (mol.g^{-1})	14.182	5.658	4.076
	k_1 (min^{-1})	0.021	0.029	0.024
Ho's pseudo-second-order	R^2	0.999	0.999	0.999
	q_e (mol.g^{-1})	12.821	12.987	12.500
	k_2 ($\text{g.mol}^{-1} \cdot \text{min}^{-1}$)	0.022	0.070	0.057

The relationship between the removal of $[\text{AuCl}_4]^-$ on MnP, MnP-HA=10:1 and 10:3 at the equilibrium as shown in Figure 8. The removal was rapid at the initial concentration from 0 to 40 mg L^{-1} . The removal was then

constant or decreased when the applied concentration of $[\text{AuCl}_4]^-$ was between 40 and 150 mg L^{-1} .

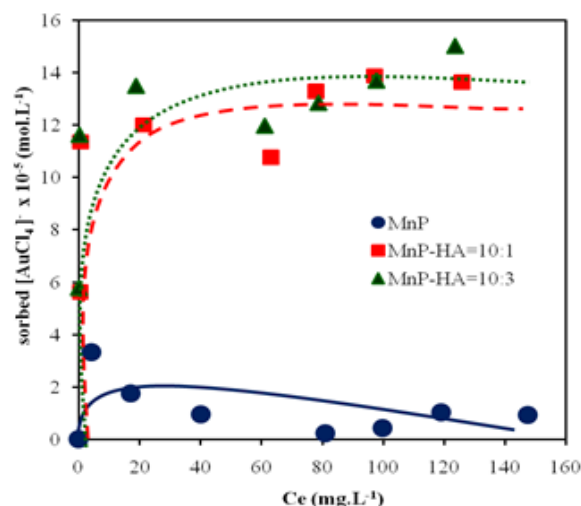


Figure 8. Relationship between removal $[\text{AuCl}_4]^-$ and $[\text{AuCl}_4]^-$ concentration at the equilibrium

To determine the sorption capacity of MnP, MnP-HA=10:1 and 10:3 to removal $[\text{AuCl}_4]^-$ were varied various of initial $[\text{AuCl}_4]^-$ concentration and the data of $[\text{AuCl}_4]^-$ sorbed at equilibrium (m , mol.g^{-1}) and the equilibrium $[\text{AuCl}_4]^-$ concentration (C_e , mol L^{-1}) were fitted to the linear form of Langmuir isotherm model, as Eq (2) [18].

$$\frac{C_e}{m} = \frac{1}{K \cdot b} t + \frac{C_e}{b} \quad (2)$$

Where b is the sorption capacity, K is the equilibrium constant (L.mol^{-1}). The result in Table 4, adsorption isotherm parameters of $[\text{AuCl}_4]^-$ on MnP, MnP-HA=10:1 and 10:3 by Langmuir and Freundlich equations. The data fit well to the model with correlation coefficients (R^2) 0.427, 0.985, and 0.983 and the sorption capacity of 0.226, 4.850, and 4.651 mol g^{-1} for MnP, MnP-HA=10:1 and 10:3 respectively.

Table 4. Adsorption isotherm parameters of $[\text{AuCl}_4]^-$ on MnP, MnP-HA=10:1 and 10:3 by Langmuir and Freundlich equations

Models	Parameters	MnP	MnP-HA=10:1	MnP-HA=10:3
Langmuir	R^2	0.427	0.985	0.983
	b (mol.g^{-1})	0.226	4.850	4.651
	K (L.mol^{-1})	0.100	0.356	0.300
	E (KJ.mol^{-1})	6.368	2.573	2.794
Freundlich	R^2	0.011	0.597	0.689
	K_f (mg.g^{-1})/(mg.L^{-1}) ⁿ	3.054	28.531	32.655
	n	18.519	10.101	12.195

4. Conclusion

Humic acid-modified magnetite (MnP-HA) was successfully done to form a bond between the carboxylic group of HA and Fe of MnP. The Coating HA on MnP unchanged the formation of the crystal structure of MnP and increased the particle size. The optimum removal of $[\text{AuCl}_4]^-$ on MnP and MnP-HA=10:1 and 10:3 were optimum at pH 3.0 and followed the Langmuir isotherm model well. The adsorption rate of removal of $[\text{AuCl}_4]^-$ on MnP-HA was higher than the bare MnP.

Acknowledgment

We gratefully acknowledge the Islamic Development Bank-Universitas Mulawarman (IDB-UNMUL) for providing financial support for this research.

References

- [1] Yusuke Kihara, Kazuto Sazawa, Hideki Kuramitz, Masaaki Kurasaki, Takeshi Saito, Toshiyuki Hosokawa, M. Suhaemi Syawal, Linda Wulandari, I. Hendri, Shunitz Tanaka, Effects of peat fires on the characteristics of humic acid extracted from peat soil in Central Kalimantan, Indonesia, *Environmental Science and Pollution Research*, 22, 4, (2015), 2384–2395
<https://doi.org/10.1007/s11356-014-2929-1>
- [2] Susan Libes, *Introduction to marine biogeochemistry*, Academic Press, 2011
- [3] Jia Li, Hongzhou Lu, Jie Guo, Zhenming Xu, Yaohe Zhou, Recycle technology for recovering resources and products from waste printed circuit boards, *Environmental Science & Technology*, 41, 6, (2007), 1995–2000 <https://doi.org/10.1021/es0618245>
- [4] P. F. Sorensen, Gold recovery from carbon-in-pulp eluates by precipitation with a mineral acid I. Precipitation of gold in eluates contaminated with base metals, *Hydrometallurgy*, 21, 2, (1988), 235–241
[https://doi.org/10.1016/0304-386X\(88\)90008-4](https://doi.org/10.1016/0304-386X(88)90008-4)
- [5] Carmen P. Gomes, Manuel F. Almeida, José M. Loureiro, Gold recovery with ion exchange used resins, *Separation and Purification Technology*, 24, 1–2, (2001), 35–57
[https://doi.org/10.1016/S1383-5866\(00\)00211-2](https://doi.org/10.1016/S1383-5866(00)00211-2)
- [6] Francisco José Alguacil, Paloma Adeva, M. Alonso, Processing of residual gold (III) solutions via ion exchange, *Gold Bulletin*, 38, 1, (2005), 9–13
<https://doi.org/10.1007/BF03215222>
- [7] R. Ranjbar, M. Naderi, H. Omidvar, Gh. Amoabediny, Gold recovery from copper anode slime by means of magnetite nanoparticles (MNPs), *Hydrometallurgy*, 143, (2014), 54–59
<https://doi.org/10.1016/j.hydromet.2014.01.007>
- [8] Feng W John Thomas, Barry Crittenden, *Adsorption technology and design*, Butterworth-Heinemann, 1998
- [9] Nan Wang, Lihua Zhu, Dali Wang, Mingqiong Wang, Zhifen Lin, Heqing Tang, Sono-assisted preparation of highly-efficient peroxidase-like Fe₃O₄ magnetic nanoparticles for catalytic removal of organic pollutants with H₂O₂, *Ultrasonics Sonochemistry*, 17, 3, (2010), 526–533
<https://doi.org/10.1016/j.ultsonch.2009.11.001>
- [10] M. Faraji, Y. Yamini, M. Rezaee, Magnetic nanoparticles: synthesis, stabilization, functionalization, characterization, and applications, *Journal of the Iranian Chemical Society*, 7, 1, (2010), 1–37
<https://doi.org/10.1007/BF03245856>
- [11] Ritu D. Ambashta, Mika Sillanpää, Water purification using magnetic assistance: a review, *Journal of Hazardous Materials*, 180, 1–3, (2010), 38–49 <https://doi.org/10.1016/j.jhazmat.2010.04.105>
- [12] Jung Kwon Oh, Jong Myung Park, Iron oxide-based superparamagnetic polymeric nanomaterials: design, preparation, and biomedical application, *Progress in Polymer Science*, 36, 1, (2011), 168–189
<https://doi.org/10.1016/j.progpolymsci.2010.08.005>
- [13] Ligang Chen, Ting Wang, Jia Tong, Application of derivatized magnetic materials to the separation and the preconcentration of pollutants in water samples, *TrAC Trends in Analytical Chemistry*, 30, 7, (2011), 1095–1108
<https://doi.org/10.1016/j.trac.2011.02.013>
- [14] K. Petcharoen, A. J. M. S. Sirivat, Synthesis and characterization of magnetite nanoparticles via the chemical co-precipitation method, *Materials Science and Engineering: B*, 177, 5, (2012), 421–427
<https://doi.org/10.1016/j.mseb.2012.01.003>
- [15] D. Maity, D. C. Agrawal, Synthesis of iron oxide nanoparticles under oxidizing environment and their stabilization in aqueous and non-aqueous media, *Journal of Magnetism and Magnetic Materials*, 308, 1, (2007), 46–55
<https://doi.org/10.1016/j.jmmm.2006.05.001>
- [16] Ling Zhang, Rong He, Hong-Chen Gu, Oleic acid coating on the monodisperse magnetite nanoparticles, *Applied Surface Science*, 253, 5, (2006), 2611–2617
<https://doi.org/10.1016/j.apsusc.2006.05.023>
- [17] Soerja Koesnarpadi, Sri Juari Santosa, Dwi Siswanta, Bambang Rusdiarso, Humic acid coated Fe₃O₄ nanoparticle for phenol sorption, *Indonesian Journal of Chemistry*, 17, 2, (2017), 274–283
<https://doi.org/10.22146/ijc.22545>
- [18] Erzsébet Illés, Etelka Tombácz, The role of variable surface charge and surface complexation in the adsorption of humic acid on magnetite, *Colloids and Surfaces A: Physicochemical and Engineering Aspects*, 230, 1–3, (2003), 99–109
<https://doi.org/10.1016/j.colsurfa.2003.09.017>
- [19] Erzsébet Illés, Etelka Tombácz, The effect of humic acid adsorption on pH-dependent surface charging and aggregation of magnetite nanoparticles, *Journal of Colloid and Interface Science*, 295, 1, (2006), 115–123
<https://doi.org/10.1016/j.jcis.2005.08.003>
- [20] Sri Juari Santosa, Shinta Rosalia Dewi, Dwi Siswanta, Eko Sri Kunarti, Esterification of Humic and its Effect on the Removal of AuCl₄⁻ from Aqueous Solution, *Journal of Ion Exchange*, 25, 4, (2014), 151–154 <https://doi.org/10.5182/jaie.25.151>
- [21] Sri Sudiono, Mustika Yuniarti, Dwi Siswanta, Eko Sri Kunarti, Triyono Triyono, Sri Juari Santosa, The Role of Carboxyl and Hydroxyl Groups of Humic Acid in Removing AuCl₄⁻ from Aqueous Solution, *Indonesian Journal of Chemistry*, 17, 1, (2017), 95–104
<https://doi.org/10.22146/ijc.23620>
- [22] Philip Anggo Krisbiantoro, Sri Juari Santosa, Eko Sri Kunarti, Synthesis of Fulvic Acid-Coated Magnetite (Fe₃O₄-FA) and Its Application for the Reductive Adsorption of [AuCl₄]⁻, *Indonesian Journal of Chemistry*, 17, 3, (2017), 453–460
<https://doi.org/10.22146/IJC.24828>
- [23] Frank J. Stevenson, *Humus chemistry: genesis, composition, reactions*, John Wiley & Sons, 1994
- [24] Liang Peng, Pufeng Qin, Ming Lei, Qingru Zeng, Huijuan Song, Jiao Yang, Jihai Shao, Bohan Liao, Jidong Gu, Modifying Fe₃O₄ nanoparticles with humic acid for removal of Rhodamine B in water,

- Journal of Hazardous Materials*, 209, (2012), 193–198
<https://doi.org/10.1016/j.jhazmat.2012.01.011>
- [25] Shen Wu, Aizhi Sun, Fuqiang Zhai, Jin Wang, Wenhuan Xu, Qian Zhang, Alex A. Volinsky, Fe₃O₄ magnetic nanoparticles synthesis from tailings by ultrasonic chemical co-precipitation, *Materials Letters*, 65, 12, (2011), 1882–1884
<https://doi.org/10.1016/j.matlet.2011.03.065>
- [26] Xian Zhang, Panyue Zhang, Zhen Wu, Ling Zhang, Guangming Zeng, Chunjiao Zhou, Adsorption of methylene blue onto humic acid-coated Fe₃O₄ nanoparticles, *Colloids and Surfaces A: Physicochemical and Engineering Aspects*, 435, (2013), 85–90
<https://doi.org/10.1016/j.colsurfa.2012.12.056>
- [27] Sri Juari Santosa, Philip Anggo Krisbiantoro, Mustika Yuniarti, Soerja Koesnarpardi, Magnetically separable humic acid-functionalized magnetite for reductive adsorption of tetrachloroaurate (III) ion in aqueous solution, *Environmental Nanotechnology, Monitoring & Management*, 15, (2021), 1–10
<https://doi.org/10.1016/j.enmm.2021.100454>
- [28] Pavel Janoš, Martin Kormunda, František Novák, Ondřej Životský, Jitka Fuitová, Věra Pilařová, Multifunctional humate-based magnetic sorbent: Preparation, properties and sorption of Cu (II), phosphates and selected pesticides, *Reactive and Functional Polymers*, 73, 1, (2013), 46–52
<https://doi.org/10.1016/j.reactfunctpolym.2012.09.001>
- [29] Yuh-Shan Ho, Gordon McKay, Pseudo-second order model for sorption processes, *Process Biochemistry*, 34, 5, (1999), 451–465
[https://doi.org/10.1016/S0032-9592\(98\)00112-5](https://doi.org/10.1016/S0032-9592(98)00112-5)